University of Pennsylvania
ScholarlyCommons

Departmental Papers (CBE)

Department of Chemical & Biomolecular Engineering

June 2008

PdZnAl Catalysts for the Reactions of Water-Gas-Shift, Methanol Steam Reforming, and Reverse-Water-Gas-Shift

R. A. Dagle
Pacific Northwest National Laboratory

A. Platon
Pacific Northwest National Laboratory

D. R. Palo
Pacific Northwest National Laboratory

A. K. Datye
University of New Mexico

John M. Vohs
University of Pennsylvania, vohs@seas.upenn.edu

See next page for additional authors

Follow this and additional works at: http://repository.upenn.edu/cbe_papers

PdZnAl Catalysts for the Reactions of Water-Gas-Shift, Methanol Steam Reforming, and Reverse-Water-Gas-Shift

Abstract

Pd/ZnO/Al$_2$O$_3$ catalysts were studied for water-gas-shift (WGS), methanol steam reforming, and reverse-water-gas-shift (RWGS) reactions. WGS activity was found to be dependent on the Pd:Zn ratio with a maximum activity obtained at approximately 0.50, which was comparable to that of a commercial Pt-based catalyst. The catalyst stability was demonstrated for 100 hours time-on-stream at a temperature of 360°C without evidence of metal sintering. WGS reaction rates were approximately 1st order with respect to CO concentration, and kinetic parameters were determined to be E$_a$ = 58.3 kJ mol^{-1} and k$_0$ = 6.1x10^7 min^{-1}. During methanol steam reforming, the CO selectivities were observed to be lower than the calculated equilibrium values over a range of temperatures and steam/carbon ratios studied while the reaction rate constants were approximately of the same magnitude for both WGS and methanol steam reforming. These results indicate that although Pd/ZnO/Al$_2$O$_3$ are active WGS catalysts, WGS is not involved in methanol steam reforming. RWGS rate constants are on the order of about 20 times lower than that of methanol steam reforming, suggesting that RWGS reaction could be one of the sources for small amount of CO formation in methanol steam reforming.

Author(s)

R. A. Dagle, A. Platon, D. R. Palo, A. K. Datye, John M. Vohs, and Y. Wang

PdZnAl Catalysts for the Reactions of Water-Gas-Shift, Methanol Steam Reforming, and Reverse-Water-Gas-Shift

Submitted to Applied Catalysis A: General

R.A. Dagle[1], A.Platon[1], D.R. Palo[1], A.K.Datye[2], J.M.Vohs[3], Y.Wang[1,*]

[1]*Pacific Northwest National Laboratory, Richland, WA 99354, USA*
[2]*Department of Chemical and Nuclear Engineering, University of New Mexico,MSC 01 1120, Albuquerque, NM 87131-0001, USA*
[3]*Department of Chemical and Bimolecular Engineering, University of Pennsylvania, Philadelphia, Pa 19104, USA*

November 28, 2007
Revised on Feb.21, 2008

* Corresponding author: Email addresses: yongwang@pnl.gov

Abstract

Pd/ZnO/Al$_2$O$_3$ catalysts were studied for water-gas-shift (WGS), methanol steam reforming, and reverse-water-gas-shift (RWGS) reactions. WGS activity was found to be dependent on the Pd:Zn ratio with a maximum activity obtained at approximately 0.50, which was comparable to that of a commercial Pt-based catalyst. The catalyst stability was demonstrated for 100 hours time-on-stream at a temperature of 360^{0}C without evidence of metal sintering. WGS reaction rates were approximately 1st order with respect to CO concentration, and kinetic parameters were determined to be E$_a$ = 58.3 kJ mol^{-1} and k$_0$ = 6.1x10^7 min^{-1}. During methanol steam reforming, the CO selectivities were observed to be lower than the calculated equilibrium values over a range of temperatures and steam/carbon ratios studied while the reaction rate constants were approximately of the same magnitude for both WGS and methanol steam reforming. These results indicate that although Pd/ZnO/Al$_2$O$_3$ are active WGS catalysts, WGS is not involved in methanol steam reforming. RWGS rate constants are on the order of about 20 times lower than that of methanol steam reforming, suggesting that RWGS reaction could be one of the sources for small amount of CO formation in methanol steam reforming.

Key words: PdZnAl catalyst, water-gas-shift (WGS), methanol steam reforming, reverse-water-gas-shift, fuel processing.

1. Introduction

As fuel cell research and development has become a flourishing area in recent years, fuel processing, including hydrogen generation, purification, and storage, is drawing a great deal of attention. Fuel cell systems are being developed for several applications, including distributed and portable power generation and other consumer applications [1-3]. Reforming of hydrocarbons is typically conducted at high temperatures, and water-gas-shift (WGS) is normally required to reduce the CO concentration in the reformate from as high as 15% down to 1-2% [4]. WGS technology for large scale applications is a well-established commercial process. The WGS reaction (1) is an equilibrium controlled, mildly exothermic reaction:

$$CO + H_2O \leftrightarrow CO_2 + H_2 \qquad \Delta H^0 = -41.1 \text{ kJ/mol} \qquad (1)$$
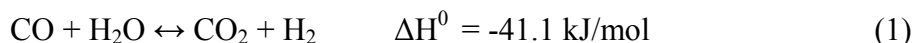
For conventional industrial applications two types of WGS catalysts are used. Fe-based high-temperature-shift (HTS) catalysts typically operate around 400-550^{0}C. Because these catalysts are less susceptible to poisons, it is preferable to convert the bulk of the CO at higher temperatures for many commercial applications [5]. A more active Cu-based catalyst is typically used as a low-temperature shift (LTS) catalyst at 200–250^{0}C [5]. Conventional WGS catalysts are not seen as attractive options for small-to-medium scale fuel cell systems. Fe-based HTS catalysts are far too inactive and pose serious volume and weight restraints. Cu-based LTS catalysts are very active at lower temperatures, but they become unstable at higher temperatures (>280^{0}C) and their pyrophoric nature makes them undesirable for safe and efficient operation [6]. Interest in WGS technology has grown significantly over the last few years as a result of recent advancements in fuel cell technology and the need to develop advanced fuel processors for conversion of hydrocarbon fuels into hydrogen. Several catalyst types have been studied as potential alternatives.

The most promising types of WGS catalysts, and those most extensively studied, have been Pt-CeO_2 based [6-9]. However, instability of this catalyst under fuel processing conditions has been a recurring problem [8-10]. There is much debate over what deactivation mechanisms are actually involved, and research on the Pt-CeO_2 based catalyst continues with a particular emphasis on increasing catalytic activity and stability.

Recently, a PdZn alloy catalyst was shown to have the activity and selectivity for methanol steam reforming comparable to that of Cu based catalysts [11-13], while it differs significantly from that of metallic Pd [14-20]. While Pd predominantly produces CO and H_2 (methanol decomposition, reaction 2), the main products are CO_2 and H_2 (methanol steam reforming, reaction 3) on the PdZn alloy catalyst. More importantly, the PdZn alloy catalyst exhibits improved thermal stability [13]. Previous studies also reported that PdZn is not only highly active for methanol reforming, but also for other reactions such as dehydrogenation/coupling of methanol to acetic acid [12] and methanol oxidation [21, 22]. Tsai et al. reported that an explanation for the identical catalytic function for PdZn and Cu is due to the fact that PdZn exhibits a similar valence electron density of states as pure Cu [23]. In a separate study by Neyman et al, the valence band spectrum of the PdZn alloy was found to resemble closely the spectrum of Cu (111), in good agreement with the calculated density of states for a PdZn alloy of 1:1 stoichiometry and implying close similarities in the reactivity of PdZn and Cu [24]. Since Cu possesses excellent WGS reactivity, it has prompted us to evaluate the WGS activity of PdZn alloy catalyst which may potentially be more stable at elevated temperatures.

$$CH_3OH \rightarrow CO + 2H_2 \qquad \Delta H^0 = 92.0 \text{ kJ/mol} \qquad (2)$$
$$CH_3OH + H_2O \rightarrow CO_2 + 3H_2 \qquad \Delta H^0 = 49.5 \text{ kJ/mol} \qquad (3)$$

This paper focuses on some recent findings that suggest the PdZnAl type catalyst which, up until now has exclusively been developed for the methanol steam reforming reaction, also appears to be active for the WGS reaction. Kinetic comparisons for the WGS, methanol steam reforming (SR), and reverse-water-gas shift (RWGS) rates were made to identify the potential roles of WGS and RWGS in the methanol steam reforming reaction.

2. Experimental

Al_2O_3 supported Pd-ZnO catalysts were prepared using a one-step co-impregnation method. Specifically, a concentrated palladium nitrate solution (20.19 wt% Pd, Engelhard Corp.) was mixed with $Zn(NO_3)_2 \bullet 6H_2O$ (99.5%, Aldrich) at 60^oC. A neutral γ-Al_2O_3 support (Engelhard Corp.) with a BET surface area of 230 m^2 g^{-1} was pre-calcined at 500^oC for 2 hrs and kept at 110^oC prior to the incipient-wetness impregnation step. The support was impregnated at 60^oC with an appropriate amount of the pre-mixed Pd and Zn nitrate solution to obtain the final products with various Pd loadings (7.3 to 13.2 wt%) and Pd/Zn molar ratios (0.25 to 0.76) while keeping the total weight percentage of Pd and Zn constant (25wt%). The wet sample was kept at 60^oC for 1 hour before drying in air at 110^oC overnight. The dried sample was then calcined at 350^oC for 3 hours. For comparison purposes, a commercial LTS CuZnAl catalyst and Pt-metal based WGS catalyst were also studied.

WGS activity tests were conducted in a 7-mm ID fixed-bed quartz tube reactor at ambient pressure. Two K-type thermocouples were installed in the reactor for the measurement of inlet and catalyst bed temperatures. Catalyst (0.100 g) was mixed with 0.500 g SiC (inert dilutent) to maintain isothermal conditions, and placed in the reactor. The catalyst was reduced using 10% H_2/Ar gas mixture at 400^oC for 2 hours prior to the test. Feed to the test bed was a gas blend intended to simulate effluent from a propane wet partial oxidation reactor. A pre-mixed gas containing 14.5% CO, 3.6% CO_2, 35.8% H_2, and 46.1% N_2 (Matheson) was introduced into the system using a mass flow controller (Brooks 5850E series). The dry pre-mixture was mixed with water in a vaporizer at 200^oC before being introduced to the reactor. Water was fed using a syringe pump (Cole Parmer 74900 series). Unless otherwise reported, the resulting wet feed mixture contained 31.6% H_2, 12.6% CO, 3.2% CO_2, 12.6% H_2O, and 40.0% N_2. A condenser and a desiccant bed were used to dry the product stream before analysis. The gaseous effluent was analyzed using a micro-GC (MTI) equipped with MS-5A and PPQ columns and a thermal conductivity detector.

Methanol steam reforming and kinetic rate tests were conducted using the same experimental setup. Using a syringe pump, pre-mixed H_2O/CH_3OH solutions were introduced into the vaporizer and reactor for reforming tests. WGS kinetic rate measurements were conducted by feeding an equimolar mixture of CO and H_2O. A syringe pump was used for the water introduction. RWGS kinetic rate measurements were conducted by feeding an equimolar mixture of CO_2 and H_2.

A JEOL 2010 high-resolution transmission electron microscope (TEM) was used to obtain the microstructures of samples. Small amounts of powder catalysts were first embedded in a hard grade LR white resin and cured at 60ºC for 6 hrs. The hardened polymer bars were sectioned into 50 nm thick slices and collected onto copper grids with Formvar/carbon support film.

3. Results and Discussion

3.1. The effects of Pd loading and Pd/Zn ratio on the WGS reaction

Similar to a previously conducted study of methanol steam reforming catalyst [11], a series of catalysts with various Pd loadings and Pd:Zn ratios were prepared on a high surface area Al_2O_3 support. Catalyst composition information is shown in Table 1. For each sample, the total amount of Pd and Zn on the Al_2O_3 support was kept constant at 25wt% while the ratio of Pd:Zn was varied. Catalytic activity comparisons were made using a feed blend representing typical effluent from that of a propane wet partial oxidation reaction. This resulting WGS feed composition as stated above was used at a GHSV of 40,000 hr^{-1}. These conditions simulate a relatively fast throughput and demanding shift requirements, which include a low H_2O:CO ratio (~1.0) and high CO:CO_2 ratio (~4.0). Figure 1 shows the CO conversion as a function of Pd:Zn molar ratio at a reaction temperature of 325ºC. While CO conversion slightly increases with the Pd:Zn ratio from 0.28 to 0.50, a sharp decrease in CO conversion from 47% to 24% was observed when Pd:Zn ratio increases from 0.50 to 0.76. However, there may be an optimum in activity around Pd:Zn = 0.50 whereas for higher ratios conversion dramatically decreases.

As we reported previously using XRD and TEM characterizations, crystallinity of PdZn alloy increases with the Pd:Zn ratio and metallic Pd was found in the catalysts with a Pd:Zn ratio of 0.76 [11]. It is also well known that metallic Pd on Al_2O_3 alone is not active for WGS [25]. Therefore, it is reasonable to attribute the initial increase in CO conversion with the Pd:Zn ratio to the increased level of PdZn alloy in the catalysts (Figure 1). At a Pd:Zn ratio >0.5 such as in the case of PdZnAl-0.76, the surface composition of PdZn alloy may deviate from an optimum Pd/Zn ratio. Another possibility is that the presence of metallic Pd may dilute the amount of surface PdZn alloy and explain the drop in CO conversion since metallic Pd alone is not very active for WGS.

It should be noted that this series of catalysts were also very selective towards CO_2. No methanation was observed (with a GC detection limit of 300 ppm) for the entire temperature range investigated, up to 400^0C. While on the Pt/CeO_2 catalysts, it has been reported that methane formation begins to occur at temperatures $>375^0C$ under WGS conditions [6, 25].

For the most active WGS catalyst found in this series, PdZnAl-0.50, the 1st order WGS kinetics with respect to CO was assumed. The rate constants as a function of temperature are depicted in Figure 2. From Figure 2, kinetic parameters were determined to be: E_a=58.3 kJ/mol, k_0=6.1X10^7 min^{-1}.

3.2. Comparison to commercial precious metal based catalyst
Activity performance for the PdZnAl-0.50 is compared to both a commercial Cu-based low-temperature shift (LTS) catalyst and a commercial Pt-based WGS catalyst, as shown in Figure 3. The same feed composition as that in Figure 1 was used, however, at a lower space velocity of GHSV=7660 hr^{-1} for lower temperature operation. Typically Cu-based catalysts are kept below 280^0C to minimize any potential metal sintering [6]. Under these conditions, it can be seen that the commercial Cu-based catalyst is the most active catalyst while the commercial Pt-based exhibits similar activity with the PdZnAl-0.50 catalyst. At a temperature of 238^0C, for example, the Cu-,Pt-,and PdZn-based catalysts

have conversions of approximately 78.2%, 51.3%, and 47.9% respectively.   As mentioned above, similar valence electron density between Cu and PdZn may suggest similar activities between these two catalysts. However, the activities were measured and compared under an identical GHSV which may not reflect the intrinsic activity difference between these two catalysts.

The high activity of the Cu-based catalyst is well known, but as discussed earlier, it has its drawbacks in terms of practical usage for fuel processing applications due to its high affinity for sintering at elevated temperatures and pyrophoricity in oxidizing environments [6]. The search for alternative WGS catalysts to overcome the drawbacks of Cu, such as Pt-based catalysts, has been the focal point of most recent studies. Precious metals supported on "reducible' type supports such as CeO_2 or CeO_2/ZrO_2 mixtures have been well reported [7, 26]. Although PdZn alloy catalysts have been well studied as of late for methanol steam reforming, their potential applications in WGS have not been reported in open literature to our best knowledge. In fact, reports focusing on the role that WGS plays in the methanol steam reforming mechanism have predominately confirmed that the WGS functionality is negligible [13, 27]. In this current study, it was found that the PdZnAl-0.50 catalyst exhibits excellent WGS activity, which is comparable to the Pt-Ceria based catalysts. While high initial activity is well documented, many groups have reported stability issues for the Pt-Ceria catalyst type [9, 10]. One of the objectives in this study was to obtain the preliminary information on the stability of the PdZnAl-0.50 catalyst under WGS conditions.

3.3 Stability of PdZnAl catalyst under WGS conditions
Figure 4 depicts CO conversion versus time-on-stream (TOS) comparing PdZnAl-0.50 and a commercial Pt-based catalyst. The catalysts were tested for approximately 100 hours under a relatively fast throughput of GHSV=90,000 hr^{-1} at a temperature of 360^{0}C. Initial conversions under these conditions for the PdZnAl-0.50 and Pt-based were 44.0% and 51.8%, respectively. After approximately 100hrs TOS, the conversions dropped to 38.5% and 44.0%, respectively. It can be seen that in the first few ~40 hours, there appears to be a small induction period after which PdZnAl-0.50 catalyst activity leveled

out. The commercial catalyst appeared to have a more gradual and constant deactivation. Despite initial step-wise deactivation, the PdZnAl catalyst shows promising stability even under relatively severe feed conditions – $CO:CO_2 = 4.0$ and $H_2O:CO = 1.0$. It should be noted that at each time interval shown in Figure 4 there were multiple data points taken. Each set of data were within approximately 2% experimental error.

Early reports suggested that the use of CeO_2 with Pt-based WGS catalysts would forever be problematic due to over-reduction of the ceria in highly reducing fuel processing environments [10]. Several groups have since refuted this claim[8, 28]. While some disagreement may still exist in the literature regarding the deactivation mechanism, much evidence exists to support Pt-sintering caused by CO and/or H_2O [9]. To assess potential sintering issues, TEM pictures were taken for the samples after an initial reduction and after 100hrs TOS, as represented in Figure 5(a) and Figure 5(b), respectively. The PdZn crystallite size distribution is shown in Figure 6. The freshly reduced PdZnAl-0.50 mean crystallite size was found to be 4.48 +/- 0.88 nm. After approximately 100 hours TOS, it was found to be 4.41 +/- 0.99 nm. Apparently, TEM evidence shown in Figure 5 suggests that PdZn crystallites exhibited no statistical change in size. There is also little change in the size distribution as evidenced from Figure 6. In short, there was only a relatively small and initial decrease in CO conversion over the 100 hours TOS studies and no evidence for any substantial sintering of the PdZn particles was observed on the PdZnAl-0.50 catalyst. It is possible that the initial, small decrease in conversion that was observed could be due to either the minor changes in crystallite size not quantitatively observed using a TEM counting method or restructuring of PdZn alloy under the WGS conditions.

3.4 Methanol reforming and CO equilibrium considerations
The excellent WGS activity observed on the PdZn catalysts prompted us to study the potential involvement of WGS in methanol steam reforming. A PdZnAl-0.38 catalyst was studied over a range of temperatures and $H_2O:CH_3OH$ ratios. This particular catalyst was chosen since it exhibited excellent activity for methanol steam reforming [11] while showing similar WGS activity as that of the PdZnAl-0.50 catalyst (Figure 1). Figure 7 shows the methanol conversion and CO selectivity as a function of temperature at

$H_2O:CH_3OH = 1.8$ and GHSV = 12,840 hr^{-1}. In Figure 7, it can be seen that in the temperature range of from 244^0C to 304^0C, the CO selectivity levels remain well below those dictated by thermodynamics. In Figure 8, CO selectivity is shown as a function of $H_2O:CH_3OH$ ratio at 220^0C while keeping the GHSV constant at 12,840 hr^{-1} and methanol partial pressure constant at 0.21atm. $H_2O:CH_3OH$ ratio was varied from 1.0 to 1.8 (molar). Again, CO selectivities remain well below equilibrium along the entire $H_2O:CH_3OH$ range investigated, even at $H_2O:CH_3OH = 1.0$, which is stoichiometric according to the reforming reaction (2). CO selectivities range from 1.9 to 1.2 as $H_2O:CH_3OH$ is varied from 1.0 to 1.8. These results are consistent with previous reports that CO levels well below equilibrium were observed on PdZn alloy catalysts [3, 12, 19]. Therefore, the methanol steam reforming pathway must not involve WGS. However, as this report suggests above PdZnAl is active specifically for the WGS reaction.

It can also be seen from Figure 8 that the methanol conversion does not vary with $H_2O:CH_3OH$ significantly, indicating that the effect of water partial pressure is negligible in the rate expression under these conditions. This zero order dependence confirms our previous report for a PdZn catalyst [29]. From a practical point of view, such a kinetic performance is highly desired since a high single path conversion can be achieved at close to a stoichiometric $H_2O:CH_3OH$ ratio without the need of excess steam.

3.5 Rate comparisons for SR, WGS,& RWGS reactions
In this last section we compare the rates of three reactions: 1) methanol steam reforming (SR), 2) WGS, and 3) RWGS. Additionally, a discussion of the interrelationships of WGS and RWGS involved in the methanol reforming pathway is made.

For the methanol steam reforming reaction, metallic Pd and defect PdZn alloy sites have previously been attributed to the CO formation on PdZn catalysts [16, 30]. To elucidate the potential involvement of RWGS on PdZn alloy for CO formation, kinetic rate constants were measured for the reactions comparing methanol steam reforming, WGS, and RWGS on the PdZnAl-0.38 catalyst. In Figure 9 the rate constants as a function of temperature are shown for three separately performed reactions. All three sets of

reactions were run using the integral method, using in some cases high conversions which correspond to more realistic conditions but operating below equilibrium. WGS and RWGS reactions were operated under a wide temperature range; at 220^0C, 300^0C, and 350^0C. A representative set of methanol steam reforming data is shown using temperatures ranging from 245^0C to 283^0C. Feed ratios were $CO:H_2O = 1$ for WGS and $CO_2:H_2 = 1$ for RWGS. All three reactions showed approximate 1st order dependence: 1st order in CO for WGS, 1st order in CO_2 for RWGS, and 1st order in methanol for steam reforming. First order dependence of methanol for methanol steam reforming reaction on PdZn was also reported in our previous kinetics study [29]. The rate constants found under these realistic conditions can provide a rough baseline for comparing the apparent kinetics of methanol steam reforming, WGS, and RWGS on the PdZnAl-0.38 catalyst. Trend lines using a power law regression for each reaction are shown in Figure 9 for reference.

From Figure 9 it can be seen that the rate constants for methanol steam reforming and WGS on the PdZnAl-0.38 catalyst are approximately the same whereas each are on the order of 20 times higher than RWGS, over the temperature range investigated. This may explain the role of CO formation in methanol steam reforming. As we discussed above, CO levels much less than predicted by equilibrium exist for the PdZn alloy catalyst in methanol steam reforming, suggesting a predominant reforming reaction pathway to CO_2. CO formation in methanol steam reforming has been attributed to the decomposition of methanol (reaction 2) on metallic Pd, which may be present in PdZn alloy catalysts [14-16]. It has also been reported that the TOF of methanol decomposition (reaction 2) on metallic Pd is about one order of magnitude lower than that on PdZn alloy for methanol steam reforming (reaction 3) [14, 15]. From Figure 9 it can be seen that RWGS is about one order of magnitude lower than WGS on the PdZnAl catalyst. Thus, it is apparent that RWGS rate on PdZn alloy and methanol decomposition on metallic Pd are of the same order of magnitude. Therefore, it is reasonable to also consider the RWGS on PdZn alloy catalyst as one possible reason for minor amount CO formation in methanol steam reforming in addition to methanol decomposition on metallic Pd.

Conclusions

A novel PdZnAl type catalyst was found to exhibit excellent WGS activity and stability, comparable to a commercial Pt-based catalyst. Although kinetic evaluations indicated that the WGS and methanol steam reforming rate constants are of the same order of magnitude, WGS is not involved in methanol steam reforming since less than equilibrium CO selectivities were observed over a wide range of temperatures and $H_2O:CH_3OH$ ratios studied. It was also found that the reaction rates for RWGS are approximately 20 times lower than that for methanol steam reforming on PdZn alloy, but are of the similar order of magnitudes as that for methanol decomposition on metallic Pd. These findings suggest that the minor amount CO formation in methanol steam reforming may be attributed to RWGS on PdZn alloy in addition to methanol decomposition on metallic Pd.

Acknowledgments

References

[1]   J.D. Holladay, Y. Wang, E. Jones, Chem. Rev. 104 (2004) 4767-4789.
[2]   D. Palo, R. Dagle, J. Holladay, Chem. Rev. 107 (2007) 3992-4021.
[3]   D.R. Palo, J.D. Holladay, R.A. Dagle, Y.-H. Chin, ACS Symp. Ser. 914 (2005) 209.
[4]   G. Hoogers, in: G. Hoogers (Ed.), Fuel Cell Technology Handbook, CRC Press, Boca Raton, 2003, pp. 5-1 to 5-23.
[5]   C. Satterfield, Heterogeneous Catalysis in Industrial Practice, 2 ed., Krieger Publishing Company, Malabar, Florida, 1996.
[6]   A. Ghenciu, Curr. Opin. Solid State Mater. Sci. 6 (2002) 395.
[7]   P. Panagiotopoulou, D. Kondarides, Catal. Today. 112 (2006) 49.

[8]   X. Wang, R.J. Gorte, J.P. Wagner, J. Catal. 212 (2002) 225-230.

[9]   W. Reuttinger, X. Liu, R.J. Farrauto, Applied Catalyst B: Environmental 65 (2006) 135.

[10]   J.M. Zalc, V. Sokolovskii, L. D.G., J. Catal. 206 (2002) 169-171.

[11]   G. Xia, J.D. Holladay, R.A. Dagle, E.O. Jones, Y. Wang, Chem. Eng. Technol. 28 (2005) 515-519.

[12]   N. Takezawa, N. Iwasa, Catal. Today. 36 (1997) 45.

[13]   N. Iwasa, N. Takezawa, Topics Catal. 22 (2003) 215.

[14]   N. Iwasa, K. Takahashi, S. Masuda, N. Takezawa, Catal. Let. 19 (1993) 211.

[15]   A. Karim, T. Conant, A. Datye, J. Catal. 243 (2006) 420.

[16]   R. Dagle, Y.-H. Chin, Y. Wang, Topics Catal. 46 (2007) 358.

[17]   Y.-H. Chin, R. Dagle, J. Hu, A.C. Dohnalkova, Y. Wang, Catal. Today. 77 (2002) 79-88.

[18]   Y.H. Chin, Y. Wang, R.A. Dagle, X.S. Li, Fuel Proc. Technol. 83 (2003) 193-201.

[19]   N. Iwasa, S. Masuda, N. Ogawa, N. Takezawa, Appl. Catal. A-Gen. 125 (1995) 145.

[20]   N. Iwasa, T. Mayanagi, N. Wataru, M. Arai, T. Takewasa, Appl. Catal. A-Gen. 248 (2003) 153-160.

[21]   S. Liu, K. Takahashi, K. Fuchigami, K. Uematsu, Appl. Catal. A-Gen. 299 (2006) 58-65.

[22]   M. Cubeiro, J. Fierro, Appl. Catal. A-Gen. 168 (1998) 307.

[23]   A. Tsai, S. Kameoka, Y. Ishii, J. Phys. Soc. Jap. 73 (2004) 3270.

[24]   K. Neyman, M., K.H. Lim, A. Chen, L.V. Moskaleva, A. Bayer, A. Reindl, D. Borgmann, R. Denecke, H.P. Steinruck, N. Rosch, Phys.Chem.Chem.Phys. 9 (2007) 3470.

[25]   C. Wheeler, A. Jhalani, E.J. Klein, S. Tummala, L.D. Schmidt, J. Catal. 223 (2004) 191-199.

[26]   S. Hilaire, X. Wang, T. Luo, R.J. Gorte, J. Wagner, Appl. Catal. A-Gen. 258 (2004) 271.

[27]   P. Pfeifer, K. Schubert, M.A. Liauw, G. Emig, Appl. Catal. A-Gen. 270 (2004) 174.

[28]   X. Liu, W. Ruettinger, X. Xu, Farrauto, Appliced Catalysis B: Environmental 56 (2005) 69.

[29]   C. Cao, G. Xia, J. Holladay, E. Jones, Y. Wang, Appl. Catal. A-Gen. 262 (2004) 19-29.

[30]   K.H. Lim, Z. Chen, K.M. Neyman, N. Rosch, J.Phys.Chem. B,. 110 (2006) 14890.

Table 1: Catalyst composition details for the series of PdZnAl catalysts with varied Pd:Zn ratios (as determined by calculation).

Sample ID	Pd:Zn	Pd
	(mol:mol)	(wt%)
PdZnAl-0.25	0.25	7.3
PdZnAl-0.38	0.38	8.9
PdZnAl-0.50	0.50	11.1
PdZnAl-0.76	0.76	13.2

List of Figures

Figure 3: Activity comparison of PdZnAl-0.50 to commercial Cu-based low-temperature shift (LTS) and WGS catalysts (feed composition: H_2=31.6%, CO=12.6%, CO_2=3.2%, H_2O=12.6%, N_2=40.0%; GHSV=7660 hr^{-1}).

Figure 4: Stability comparison of PdZnAl-0.50 to commercial Pt-based WGS catalyst (feed composition: H_2=31.6%, CO=12.6%, CO_2=3.2%, H_2O=12.6%, N_2=40.0%; Temperature=360^0C; GHSV=90,000 hr^{-1}; ~100 hrs TOS).

Figure 5: TEM pictures for the PdZnAl-0.50 catalyst (a) after initial reduction and (b) after 100hrs TOS (reaction feed composition: H_2=31.6%, CO=12.6%, CO_2=3.2%, H_2O=12.6%, N_2=40.0%; Temperature=360^0C; GHSV=90,000 hr^{-1}).

Figure 6: Particle size distribution from TEM analysis for the PdZnAl-0.50 catalyst after initial reduction and after 100hrs TOS (reaction feed composition: H_2=31.6%, CO=12.6%, CO_2=3.2%, H_2O=12.6%, N_2=40.0%; Temperature=360^0C; GHSV=90,000 hr^{-1}).

Figure 7: Methanol steam reforming conversion and CO selectivity temperature profiles for the PdZnAl-0.38 catalyst (GHSV=12,840 hr^{-1}, H_2O/C=1.8, P_{N2}=0.25atm).

Figure 8: Methanol conversion and CO selectivity as a function of H_2O/C (mol) feed ratio for the PdZnAl-0.38 catalyst (Temperature=220^0C. GHSV=12,840 hr^{-1}, P_{MeOH}=0.21atm, P_{N2} varied to keep constant GHSV).

Figure 9: Rate constant comparison for the PdZnAl-0.38 catalyst for the methanol steam reforming (SR), water-gas shift (WGS), and reverse-water-gas shift (RWGS) reactions as a function of temperature.

Figure 1: Effect of Pd:Zn molar ratio on CO conversion under WGS reaction conditions at 325^0C (feed composition: H_2=31.6%, CO=12.6%, CO_2=3.2%, H_2O=12.6%, N_2=40.0%; GHSV=40,000 hr^{-1}).
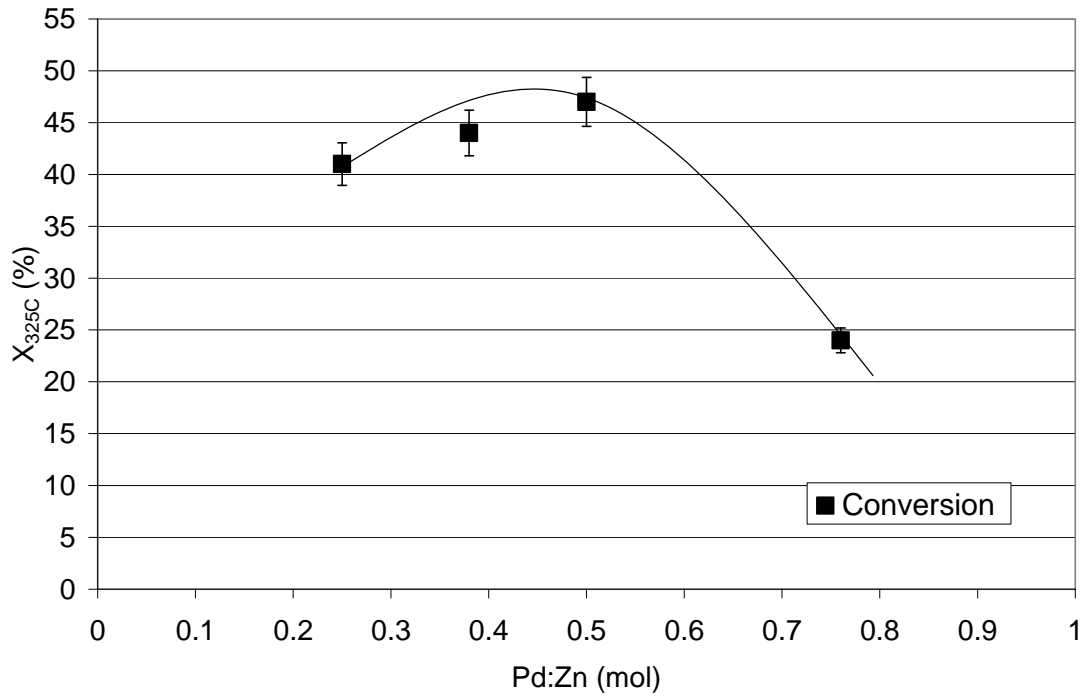
Figure 2: Arrhenius plot for the water-gas shift (WGS) reaction for the PdZnAl-0.50 catalyst, assuming 1st order kinetics (feed composition kept constant: H_2=31.6%, CO=12.6%, CO_2=3.2%, H_2O=12.6%, N_2=40.0%; temperature varied, GHSV varied =7660, 10,227, and 20,455 hr^{-1}).
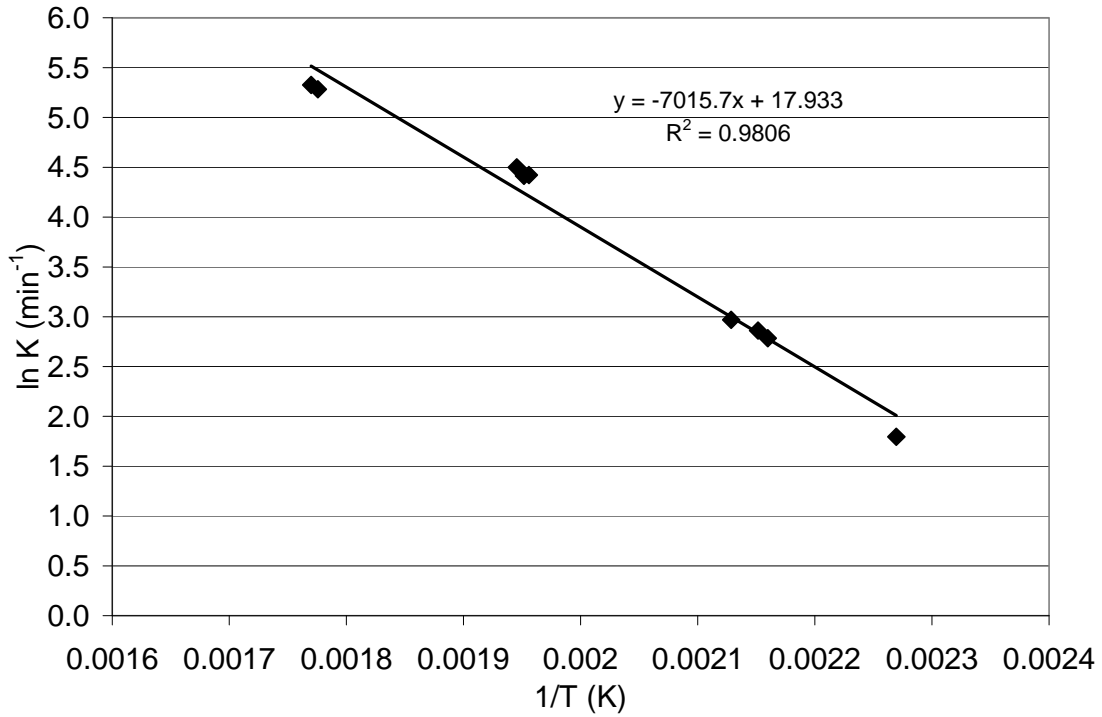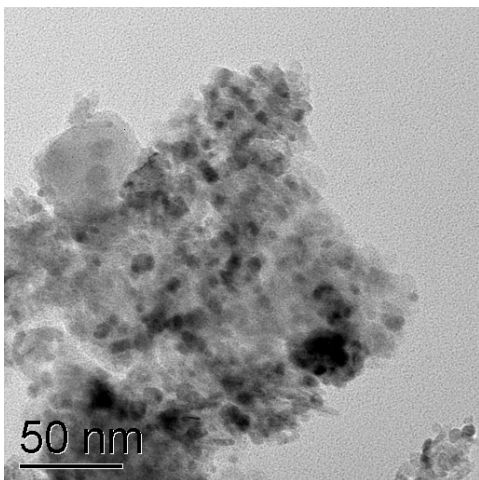

$$y = -7015.7x + 17.933$$
$$R^2 = 0.9806$$

Figure 3: Activity comparison of PdZnAl-0.50 to commercial Cu-based low-temperature shift (LTS) and commercial Pt-based WGS catalysts (feed composition: H_2=31.6%, CO=12.6%, CO_2=3.2%, H_2O=12.6%, N_2=40.0%; GHSV=7660 hr^{-1}).
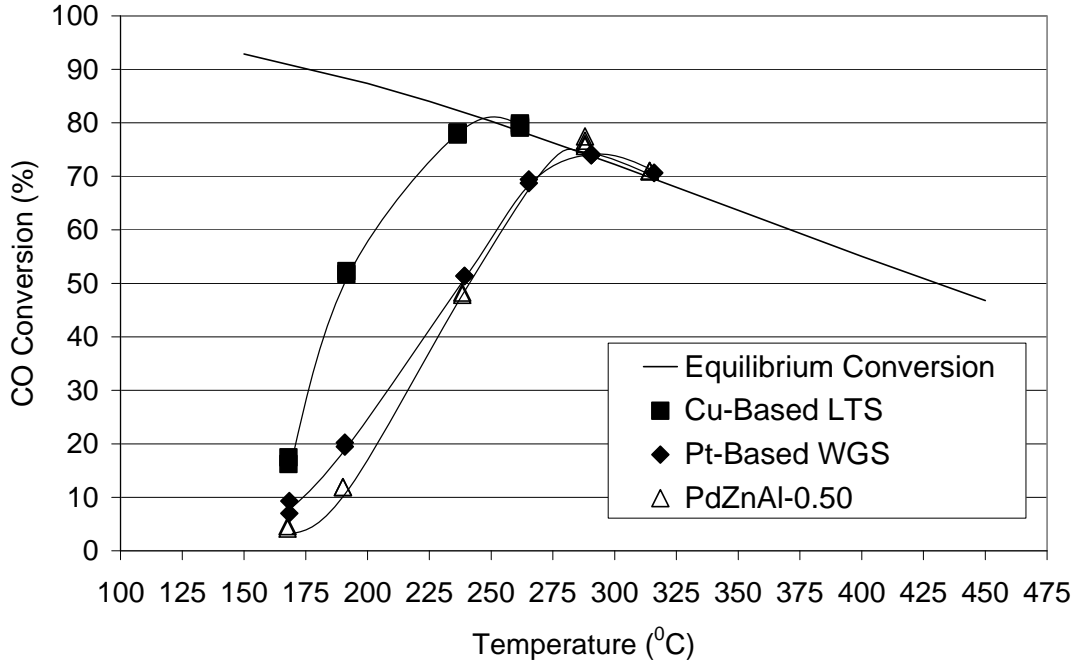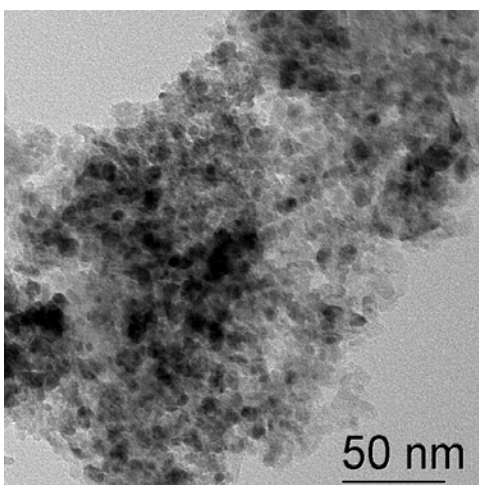
Figure 4: Stability comparison of PdZnAl-0.50 to commercial Pt-based WGS catalyst (feed composition: H_2=31.6%, CO=12.6%, CO_2=3.2%, H_2O=12.6%, N_2=40.0%; Temperature=360^{0}C; GHSV=90,000 hr^{-1}; ~100 hrs TOS).
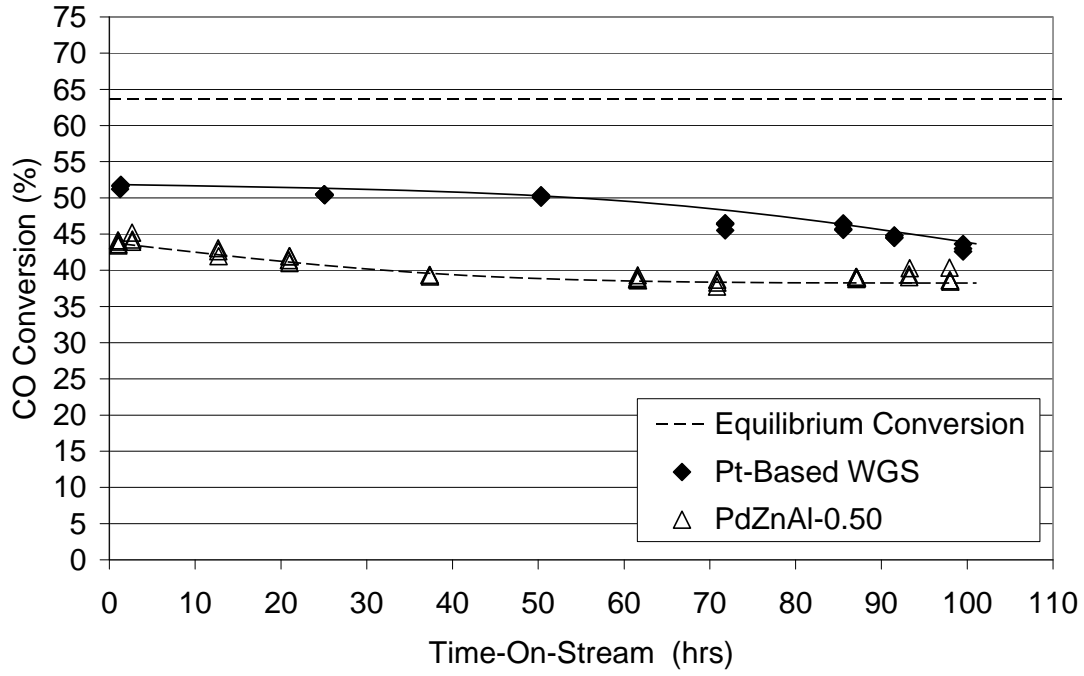
Figure 5: TEM pictures for the PdZnAl-0.50 catalyst (a) after initial reduction and (b) after 100hrs TOS (reaction feed composition: H_2=31.6%, CO=12.6%, CO_2=3.2%, H_2O=12.6%, N_2=40.0%; Temperature=360^{0}C; GHSV=90,000 hr^{-1}).
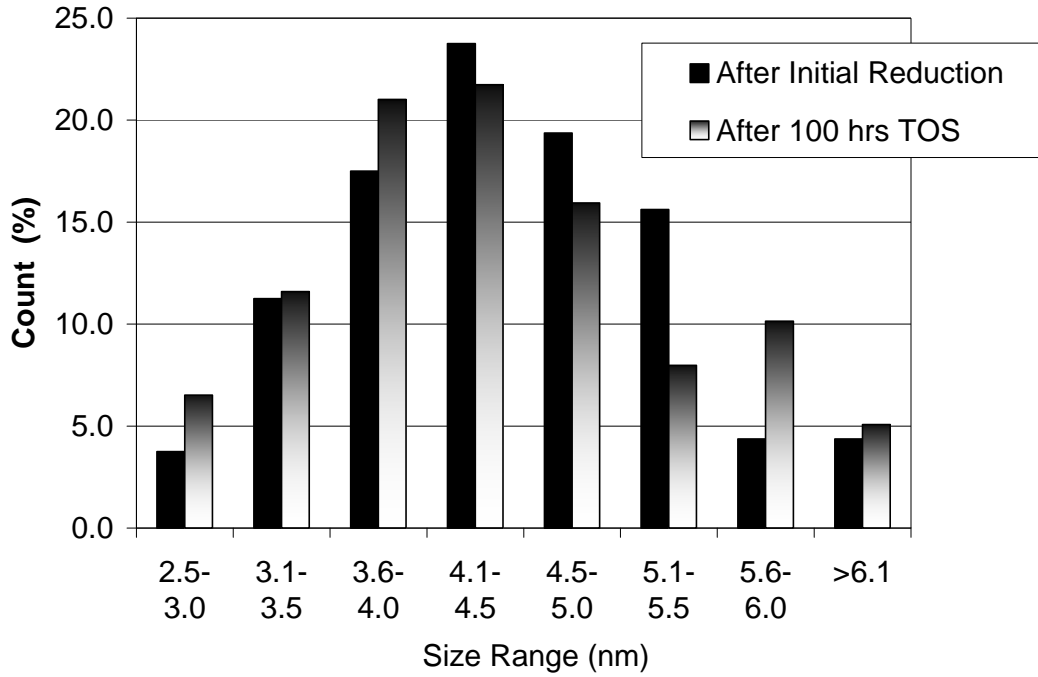

(a)

(b)

Figure 6: Particle size distribution from TEM analysis for the PdZnAl-0.50 catalyst after initial reduction and after 100hrs TOS (reaction feed composition: H_2=31.6%, CO=12.6%, CO_2=3.2%, H_2O=12.6%, N_2=40.0%; Temperature=360^{0}C; GHSV=90,000 hr^{-1}).
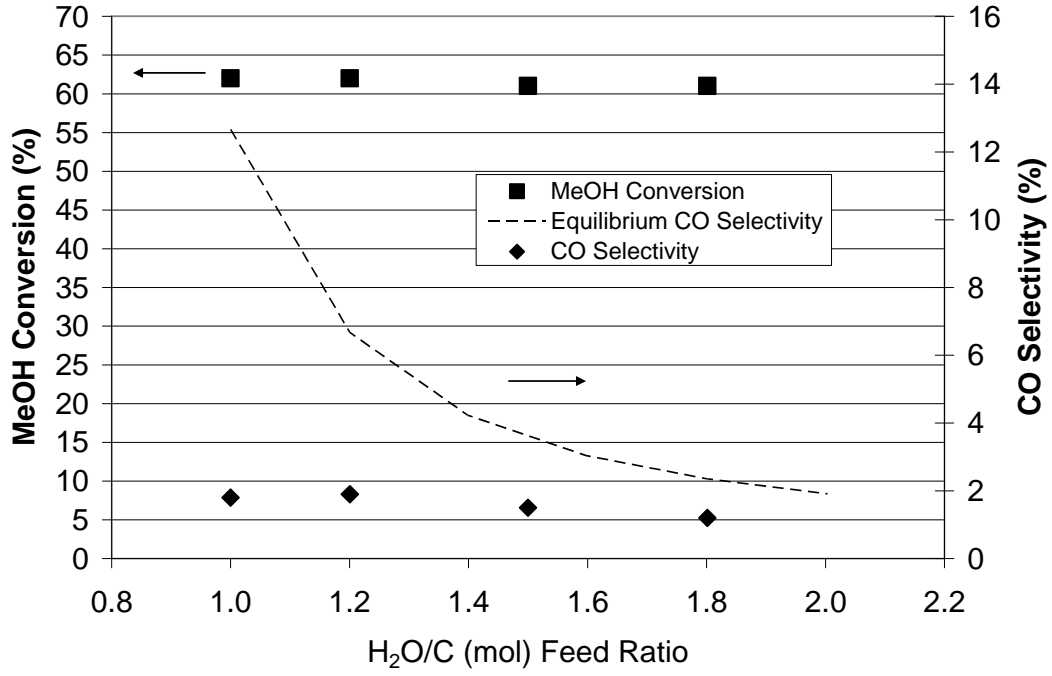
Figure 7: Methanol steam reforming conversion and CO selectivity temperature profiles for the PdZnAl-0.38 catalyst (GHSV=12,840 hr^{-1}, H_2O/C=1.8, P_{N2}=0.25atm).
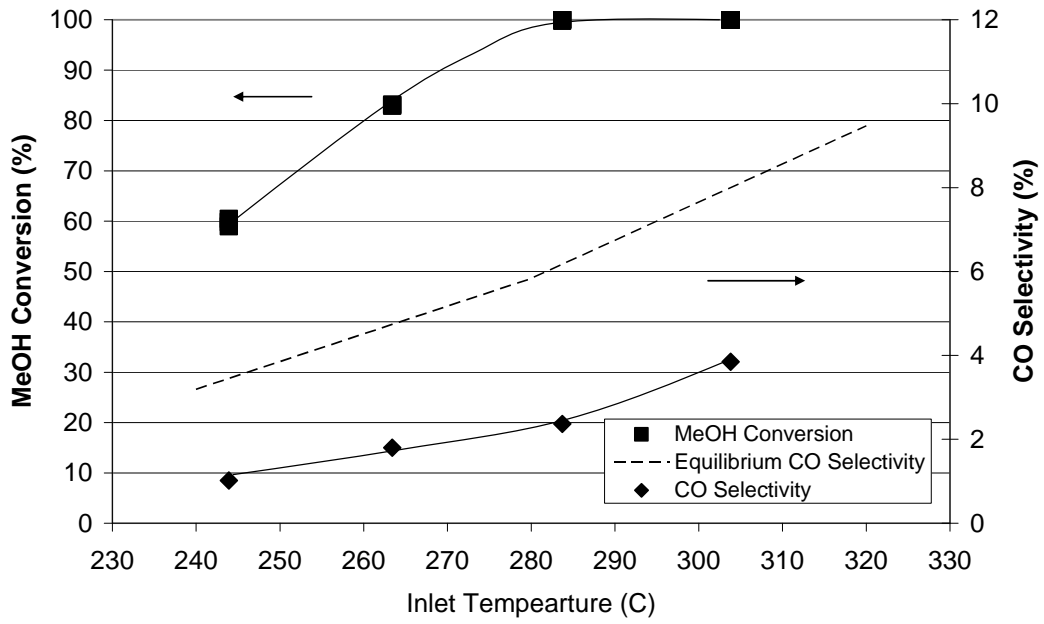
Figure 8: Methanol conversion and CO selectivity as a function of H_2O/C (mol) feed ratio for the PdZnAl-0.38 catalyst (Temperature=220^0C. GHSV=12,840 hr^{-1}, P_{MeOH}=0.21atm, P_{N2} varied to keep constant GHSV).

Figure 9: Rate constant comparisons as a function of temperature for the PdZnAl-0.38 catalyst for the methanol steam reforming (SR), water-gas shift (WGS), and reverse-water-gas shift (RWGS) reactions. Power law regression trend lines are shown for each reaction.

Figure content:
- y-axis left: k (1/min), from 1 to 10000
- y-axis right: k_{SR}/k_{RWGS}, from 0 to 25
- x-axis: Temperature (^{0}C), from 200 to 360
- $y = 8E\text{-}15x^{6.832}$
- $R^2 = 0.9837$
- $y = 3E\text{-}18x^{8.1908}$
- $R^2 = 0.9976$
- $y = 2E\text{-}16x^{7.0082}$
- $R^2 = 0.9926$
- Legend: ■ SR, ◇ WGS, ▲ RWGS, — k(SR)/k(RWGS)